Journal of the Southeastern Association for Research in Astronomy, **6**, 10-14, 2012 July 10

A STANDARD STAR SYSTEM FOR INTERMEDIATE-BAND CAH PHOTOMETRY: SARA U42A AND NURO DATA

Chelsea Spengler[1]
Department of Astronomy, Case Western Reserve University, Cleveland, OH, 44106

Laurel Farris[1]
Department of Physics, Astronomy and Material Science, Missouri State University, Springfield, MO, 65807

and

Thomas Robertson
Department of Physics and Astronomy, Ball State University, Muncie, IN, 47306

ABSTRACT

This project uses a technique to solve for four transformation coefficients simultaneously for multiple nights of observations and a nightly zeropoint value. The observed values are transformed to a standard system based on the R and $(R-I)$ Landolt standards and the instrumental $(R-L)$ (CaH) color of the U42a system on the 0.9-meter telescope operated by the Southeastern Association for Research in Astronomy (SARA). Transformation coefficients are calculated for observations of standard and program stars from the Lowell 0.78-meter telescope operated by the National Undergraduate Research Observatory (NURO). The transformed NURO standard star observations are compared to those using the U42a system. Likewise, the NURO program stars are compared to matching stars observed with SARA's U55 camera, which has also been transformed to the standard system. We find that all the observations agree well and have been successfully converted to the standard system. The implementation of this new system will allow for greater ease when separating red dwarfs and giants using the $(R-L)$ and $(R-I)$ colors, and may permit more accurate modeling of absolute magnitudes for late M dwarfs as a function of $(R-I)$.

Subject headings: methods—data analysis—astronomical databases: miscellaneous—stars: late type—stars: low-mass

1. INTRODUCTION

A large part of the stellar population in nearby areas of the Galaxy is composed of cool, faint red dwarfs. Understanding red dwarfs is integral to understanding the galaxy as a whole; however, it is difficult to identify these dwarfs without inadvertently including more luminous, but more distant, giants in the classification as well. Even once dwarfs are separated from giants, subdwarfs can result in errors in photometric parallaxes. In past research on the space density of red dwarfs, contamination from giants has resulted in uncertainty except at high galactic latitudes where distant giants are rare. Once stars are identified as main sequence stars, differences in absolute magnitude result in substantial random errors of 0.2–0.3 mag when attempting a fit to the M_R vs. $(R-I)$ diagram, resulting in random errors in subsequent photometric parallax calculations (Siegel et al. 2002). With absolute magnitude errors of 0.2–0.3 mag, the calculated distances would have errors of 10–15%. Siegel et al. also reported errors of approximately 1 and 2 mag for subdwarfs and extreme subdwarfs, respectively. Distances calculated for these stars would have errors of 45–90%. Currently stars are classified as subdwarfs or extreme subdwarfs based on metallicity, with halo stars being the most metal-poor and most likely to be a subdwarf. Once the stars were identified, Siegel et al. then used an intricate correction for the systematic distance errors to develop a better estimate of the stellar density. The introduction of a calcium hydride (CaH) filter might allow subdwarfs to be classified based on direct observation and could ultimately improve calibration for photometric parallaxes.

An intermediate-band calcium hydride (L) filter has already proven useful for separating red dwarfs and giants when the $(R-I)$ color is plotted against $(R-L)$ (Robertson & Furiak 1995; Robertson & Scott 2000; Croy et al. 2003; Matney et al. 2003; Mason et al. 2008; Mason & Robertson 2008; Humphrey & Robertson 2008; Mason 2009). These studies were based on instrumental $(r-l)$ color indices as observed on a number of photometric systems. While efforts were made to ensure that they were sufficiently similar to produce effective luminosity classes, no standard system was established and each change in camera, filters or observatory produced a slightly different set of instrumental colors. The creation of a standard $(R-L)$ color index with a system of standard stars would simplify recalibration when there are changes to the photometric system. This project is part of an effort to create such a system.

2. OBSERVATIONS

2.1. *SARA Data*

Observations using an intermediate-band L filter with the Kron-Cousins R and I colors are summarized in Table 1. The observations made with the Southeastern As-

Electronic address: ces58@case.edu
[1] Southeastern Association for Research in Astronomy (SARA) NSF-REU Summer Intern

TABLE 1
Photometric systems used for CaH photometry

Photometric System	Camera	Broad-Band *RI* Filters	CaH Filter
BSUO[a]	Photometrics Star 1	(1)	(1)
NURO	Photometrics Tek 512	(2)	(2)
U55	Apogee U55	(3)	(2)
U42a	Apogee U42	(3)	(2)
U42b	Apogee U42	(3)	(3)

Note. — Photometric systems with identical numbers in a given column used the same filter.
[a] Ball State University Observatory

sociation for Research in Astronomy (SARA) U42 camera are most extensive and have been used to establish the standard photometric system. Observations made between July 2006 and April 2007 form the system designated U42a in Table 1. Observations of standard stars from Landolt (1983, 1992) were observed and instrumental magnitudes of r and l formed the basis of the $(R-L)$ color index.

Mean extinction coefficients for $BVRI$ colors have been determined empirically for the BSU, NURO and SARA observations. Mean extinction coefficients for Kitt Peak were also published by Landolt and Uomoto Landolt & Uomoto (2007). Based on these values a mean extinction coefficient for the R filter was adopted as 0.11 mag airmass^{-1}. Given an effective wavelength of 683 nm for the CaH (L) filter, a mean extinction value of 0.10 mag airmass^{-1} was computed. All stars observed on the U42a system produced $(R-L)$ values defined by

$$(R-L) = (r - 0.11X) - (l - 0.10X) + 2.43, \qquad (1)$$

where X is the airmass of the observation. The 2.43 was added to produce an $(R-L)$ value of 0.0 when $(R-I) = 0.0$. There were 146 Landolt standard stars having $(R-L)$ values on the U42a system. These stars served as the primary standard stars for the catalog. Program stars observed on the U42a $(R-L)$ system provided additional data points to test reliability of transformations from the other photometric systems. The limited number of red dwarf standard stars and the absence of very red giant standards make supplemental red star observations quite helpful. Figure 1 shows the $(R-L)$ v. $(R-I)$ two-color diagram for the original set of standard stars.

The goal of this project is to transform the observations made at NURO to the same $(R-L)$ photometric system as defined by these standard stars. A related project (Farris, Spengler, & Robertson 2012) transformed data obtained at SARA with the U55 camera to this system and effectively increased the number of standard stars to 176.

2.2. *NURO Data*

Observations were made using the Lowell 0.78-meter telescope equipped with a Photometrics Tek 512 CCD operated by the National Undergraduate Research Observatory (NURO). A total of 14 nights with good photometry were selected for this project. The data were collected over the course of about 10 years, between November 1995 and May 2005. All nights include exposures in the Kron-Cousins R and I filters, as well as in an intermediate-band L filter centered at 683 nm with a bandwidth of 13 nm. Stars from the Landolt standard catalogs Landolt (1983, 1992) were observed each night, with some stars observed at a range of airmass values to calculate extinction coefficients. The images were reduced using IRAF[2].

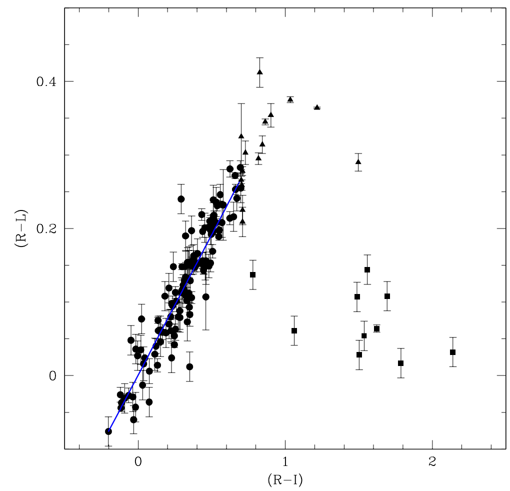

Fig. 1.— $(R-L)$ v. $(R-I)$ color-color diagram for the U42a standard system, consisting of 421 observations of 146 stars. Triangular points are red giants, squares are red dwarfs, and circles are "warm standards." The fit to these warm standards is $y = 0.38x$.

The standard star observations were then processed using the method outlined in Harris, Fitzgerald, & Reed (1981). We used this method instead of the functions available in IRAF because of its ability to process multiple nights at once. With about four or five standard stars per night, we had an insufficient number of data points to calculate meaningful nightly color coefficients. Combining the 63 stars from all of our nights produced global coefficients with reasonable errors. Due to the limitations of our data we also adopted a mean extinction coefficient to be used for all nights. Most of our nights do not have observations at a sufficient range of airmasses, and instead include more observations of program and standard stars near the meridian for optimal photometry. While this provides more data for eventual analysis, it limits how well the data can be corrected for extinction. Only a few nights contain all this information for reliable extinction coefficient calculations. Instead of computing coefficients for each night, we opted to compute one value using all the stars from all nights. While this is certainly not ideal for data collected over the course of a decade, it at least allows us to use these observations in this current project. The only parameter calculated for each night was the zeropoint coefficient, which could be computed reasonably well despite our limitations.

3. RESULTS

Values for R, $(R-I)$ and $(R-L)$ on the standard system were calculated using the following equations:

$$(r-R) = \alpha_1 + \alpha_2 X + \alpha_3(R-I) + \alpha_4 X(R-I) + \alpha_5(R-I)^2 \qquad (2)$$

[2] IRAF is distributed by the National Optical Astronomy Observatories, which are operated by the Association of Universities for Research in Astronomy, Inc., under cooperative agreement with the National Science Foundation.

TABLE 2
TRANSFORMATION COEFFICIENTS FOR R, $(R-I)$ AND $(R-L)$

Coefficient	R	$(R-I)$	$(R-L)$
ZP 1	0.368 ± 0.026	-0.199 ± 0.025	-2.635 ± 0.025
ZP 2	0.368 ± 0.025	-0.208 ± 0.024	-2.651 ± 0.023
ZP 3	0.354 ± 0.029	-0.217 ± 0.028	-2.664 ± 0.026
ZP 4	0.362 ± 0.019	-0.203 ± 0.019	-2.663 ± 0.021
ZP 5	0.114 ± 0.019	-0.265 ± 0.019	-2.655 ± 0.020
ZP 6	0.545 ± 0.019	-0.234 ± 0.019	-2.623 ± 0.020
ZP 7	0.538 ± 0.018	-0.232 ± 0.018	-2.635 ± 0.019
ZP 8	0.547 ± 0.017	-0.203 ± 0.017	-2.651 ± 0.018
ZP 9	0.837 ± 0.021	-0.231 ± 0.021	-2.616 ± 0.022
ZP 10	0.845 ± 0.019	-0.200 ± 0.019	-2.625 ± 0.021
ZP 11	0.807 ± 0.021	-0.225 ± 0.021	-2.604 ± 0.021
ZP 12	0.767 ± 0.021	-0.220 ± 0.020	-2.607 ± 0.020
ZP 13	1.903 ± 0.021	-0.154 ± 0.021	-2.589 ± 0.021
ZP 14	1.892 ± 0.020	-0.134 ± 0.020	-2.573 ± 0.020
X	0.105 ± 0.011	0.042 ± 0.011	0.078 ± 0.012
CI	0.047 ± 0.029	1.141 ± 0.028	1.708 ± 0.208
$CI * X$	0.003 ± 0.018	0.001 ± 0.017	-0.465 ± 0.124
CI^2	0.027 ± 0.011	0.051 ± 0.011	-0.134 ± 0.261

NOTE. — $ZP\ m$ denotes the zeropoint coefficient calculated for night m, X denotes the first order extinction coefficient, CI denotes the first-order color term coefficient, $CI * X$ denotes the color-extinction term coefficient, and CI^2 denotes the second-order color term coefficient.

$$(r-i) = \beta_1 + \beta_2 X + \beta_3 (R-I) + \beta_4 X (R-I) + \beta_5 (R-I)^2 \quad (3)$$

$$(r-l) = \gamma_1 + \gamma_2 X + \gamma_3 (R-L) + \gamma_4 X (R-L) + \gamma_5 (R-L)^2 \quad (4)$$

where r is the instrumental magnitude and α_i, β_i, and γ_i are the transformation coefficients for R, $(R-I)$, and $(R-L)$, respectively. The results for these transformation coefficients were then used to find magnitudes and colors on the standard system for the program stars. The results for the program stars are compared to the program stars from the U42a system and the U55 system Farris et al. (2012).

Table 2 shows the transformation coefficients and their respective errors that were calculated for this project. Note that almost all the coefficients are well-defined with relatively small errors. The exceptions to this are the color-extinction term for R and $(R-I)$ and the second-order color term for $(R-L)$. The higher errors for these terms could be due to a lack of effect from those particular parameters.

4. ANALYSIS AND DISCUSSION

Figure 2 shows the comparison of the NURO standard star $(R-L)$ and $(R-I)$ observations to those from the U42a system. Errors are ± 0.02 mag and were determined based on the standard deviation about the mean for stars with multiple observations. An ideal transformation to the standard system would remove any systematic color effects and plots of the color index differences, like those in Figure 2, would have fit lines with slopes and intercepts of zero. For Figure 2(a), the slope is -0.002 ± 0.003 and the intercept is -0.001 ± 0.004 with $\sigma = 0.024$. Likewise, for Figure 2(b), the slope is -0.003 ± 0.006 and the intercept is -0.0003 ± 0.008 with $\sigma = 0.049$. This standard deviation is higher than expected, but is most likely primarily due to the three observations that have $\Delta(R-L) \approx 0.15$. These points are all the same star observed on three consecutive nights, so it's possible there was a problem with the observations of that particular star. The possibility of cloud or weather effects during those observations exists as well, although those nights as a whole seemed to have good photometry. Based on these values we can be fairly certain that all systematic color effects have been removed and the NURO data are successfully transformed to the new system.

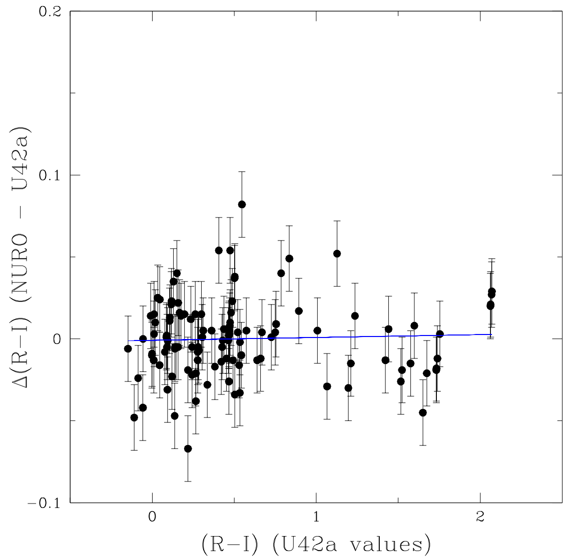

(a) $(R-I)$ differences. The fit line is $y = -0.002x - 0.001$. The data have a standard deviation of 0.024.

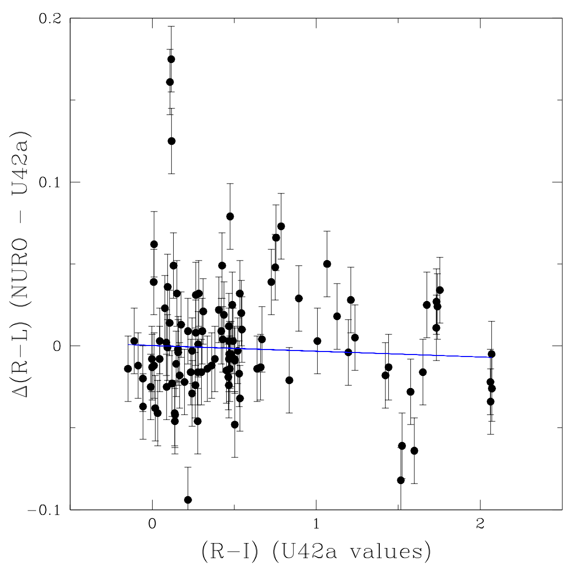

(b) $(R-L)$ differences. The fit line is $y = -0.003x - 0.0003$. The data have a standard deviation of 0.049.

FIG. 2.— Color index differences between NURO and U42a data.

Next we compared the 43 matching program stars from the NURO and U55 observations. Figure 3 shows our comparisons. These plots use the mean $(R-I)$ value calculated from the NURO and U55 observations. Errors in this value are variable but minor and typically are about 0.014 mag. Any repeated observations for a given star have been averaged into a single observation for comparison. Errors are variable but usually about ± 0.03 mag, from uncertainties in both the U55 and NURO trans-

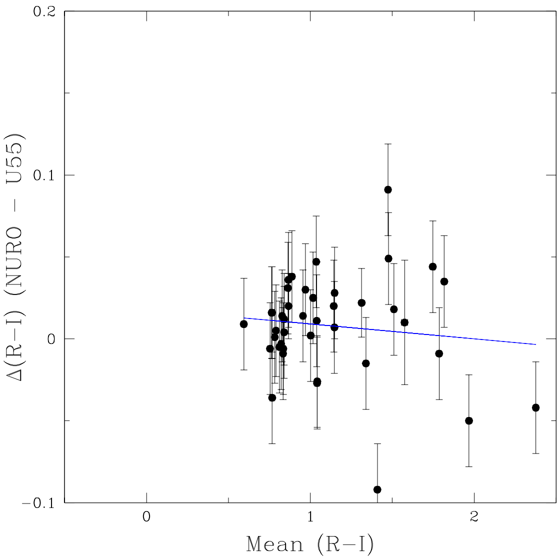

(a) $(R-I)$ differences. The fit line is $y = -0.01x - 0.02$. The data have a standard deviation of 0.032.

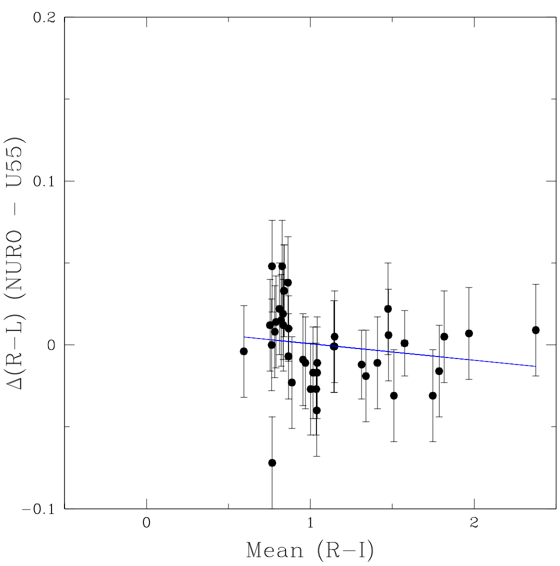

(b) $(R-L)$ differences. The fit line is $y = -0.01x - 0.01$. The data have a standard deviation of 0.025.

FIG. 3.— Color index differences between NURO and U55 data. In both plots the x-axis errors are almost smaller than the data points.

formed values. Again, we expect a slope and intercept close to zero for our fit lines. For Figure 3(a) the slope is -0.01 ± 0.01 and the intercept is 0.02 ± 0.01 with $\sigma = 0.032$. For Figure 3(b) the slope is -0.01 ± 0.01 and the intercept is 0.01 ± 0.01 with $\sigma = 0.025$. While these values are significantly higher than those for the fit with the U42a data, we still believe the U55 and NURO data agree, and both have been successfully transformed to the standard system. This fit has fewer stars, so any star with an exceptionally high residual has greater effect on the fit line than a similar star from the U42a fit.

5. CONCLUSION

The goal of this project was to transform data from NURO to the U42a standard system, including standard values for the $(R-L)$ color. We have successfully accomplished this, as shown by comparisons to both the U42a and U55 data. The next logical step is to expand the catalog. The set of standard stars is rather small, but will be increased by continued observation of other stars for which there are also data on the U42a system. Once new observations are matched to the U42a system, these stars could also be added to the catalog in the same way observations from the U55 system increased the standard catalog to 176 stars. Observations have been collected on the U42b system at SARA using a new L filter. These data may provide additional stars for the standard system, but have not yet been reduced and transformed. Part of this expansion should include gathering data from areas of the sky that currently have little to no standard star observations. As shown in Figure 4, there are very few observations for red stars, and those observations are only at a few right ascension positions. Ideally there should be many more red stars included at a larger range of right ascension values. This will make the system more useful for observations at any time of the year. It will also provide a better reference for data transformation, because the linear fit produced from bluer standard stars cannot be assumed to extend so far redward.

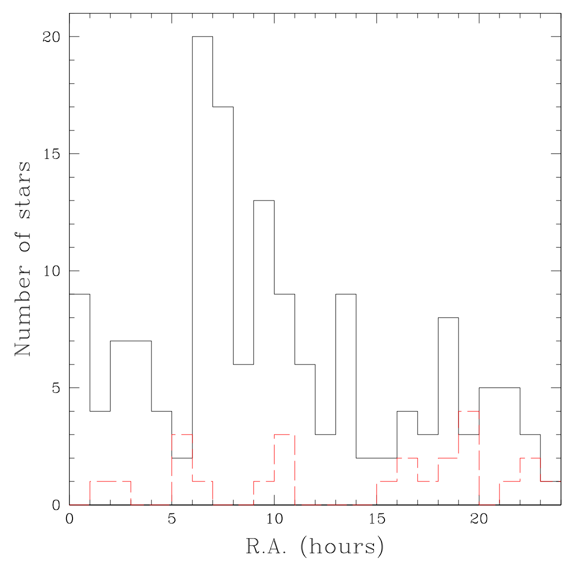

FIG. 4.— Distribution of standard stars. Very red stars (with $(R-I) > 0.7$) are shown in the dashed red histogram. All other stars are in the solid black histogram.

Another continuation of this project would be to begin applying it to red dwarfs. Ideally it should provide more accurate $(R-L)$ vs. $(R-I)$ color-color diagrams, which would allow for better separation between giants and dwarfs. Efforts are underway to try to use the $(R-L)$ color index to improve the quality of photometric parallaxes for late type dwarfs by measuring differences in chemical abundance.

This project was funded by the National Science Foundation Research Experiences for Undergraduates (REU) program through grant NSF AST-1004872 to the Florida Institute of Technology.

REFERENCES

Croy, J. R., Robertson, T. H., Jordan, T. M., Snyder, L. A., Welsh, F. V., Matney, J. E., Seaton, R. L., & Poweska, S. J. 2003, Bulletin of the American Astronomical Society, 36, #142.03

Farris, L., Spengler, C., & Robertson, T. 2012, JSARA, 6, 5

Harris, W. E., Fitzgerald, M. P., & Reed, B. C. 1981, PASP, 93, 507

Humphrey, N., & Robertson, T. 2008, Bulletin of the American Astronomical Society, 40, 204

Landolt, A. U. 1983, AJ, 88, 439

Landolt, A. U. 1992, AJ, 104, 340

Landolt, A. U., & Uomoto, A. K. 2007, AJ, 133, 768

Mason, J. 2009, Ball State University master's thesis (unpublished)

Mason, J. R., Humphrey, N., Briggs, A., Parrell, A., & Robertson, T. 2008, American Astronomical Society Meeting Abstracts #211, 211, #163.03

Mason, J. R., & Robertson, T. H. 2008, Bulletin of the American Astronomical Society, 40, 203

Matney, J. E., Robertson, T. H., Jordan, T. M., Snyder, L. A., Welsh, F. V., Croy, J. R., Poweska, S. J., & Seaton, R. E. 2003, Bulletin of the American Astronomical Society, 36, #137.03

Robertson, T. H., & Furiak, N. M. 1995, Bulletin of the American Astronomical Society, 27, 1302

Robertson, T. H., & Scott, A. 2000, Bulletin of the American Astronomical Society, 197, 421

Siegel, M. H., Majewski, S. R., Reid, I. N., & Thompson, I. B. 2002, ApJ, 578, 151